CD20-targeted tetrameric interferon-α, a novel and potent immunocytokine for the therapy of B-cell lymphomas

Edmund A. Rossi,[1] David M. Goldenberg,[2] Thomas M. Cardillo,[1] Rhona Stein,[2] and Chien-Hsing Chang[1]

[1]Immunomedics Inc, Morris Plains, NJ; and [2]Center for Molecular Medicine and Immunology, Garden State Cancer Center, Belleville, NJ

Interferon-α (IFN-α) has direct inhibitory effects on some tumors and is a potent stimulator of both the innate and adaptive immune systems. A tumor-targeting antibody-IFN-α conjugate (mAb-IFN-α) could kill by direct actions of the monoclonal antibody (mAb) and IFN-α on tumor cells and also potentiate a tumor-directed immune response. The modular Dock-and-Lock method (DNL) was used to generate 20-2b, the first immunocytokine having 4 cytokine (IFN-α2b) groups that are fused to the humanized anti-CD20 mAb, veltuzumab. Additional mAb-IFN-α constructs, each retaining potent IFN-α2b biologic activity, also were produced by DNL. The 20-2b shows enhanced antibody-dependent cellular cytotoxicity compared with veltuzumab but lacks complement-dependent cytotoxicity. The 20-2b inhibits in vitro proliferation of lymphoma cells and depletes them from whole human blood more potently than the combination of veltuzumab and a nontargeting, irrelevant, mAb-IFN-α. The 20-2b demonstrated superior therapeutic efficacy compared with veltuzumab or nontargeting mAb-IFN-α in 3 human lymphoma xenograft models, even though mouse immune cells respond poorly to human IFN-α2b. Targeting IFN-α with an anti-CD20 mAb makes the immunocytokine more potent than either agent alone. These findings suggest that 20-2b merits clinical evaluation as a new candidate antilymphoma therapeutic. (Blood. 2009;114: 3864-3871)

Introduction

Multiple studies have shown that interferon-α (IFN-α) can have antitumor activity in both animal models[1-3] and cancer patients.[4] IFN-α can exert a variety of direct antitumor effects, including down-regulation of oncogenes, up-regulation of tumor suppressors, enhancement of immune recognition via increased expression of tumor surface major histocompatibility complex class I proteins, potentiation of apoptosis, and sensitization to chemotherapeutic agents.[5-9] For some tumors, IFN-α can have a direct and potent antiproliferative effect through activation of STAT1.[10] Indirectly, IFN-α can inhibit angiogenesis[11] and stimulate host immune cells, which may be vital to the overall antitumor response but has been largely underappreciated.[12] IFN-α has a pleiotropic influence on immune responses through effects on myeloid cells,[13,14] T cells,[15,16] and B cells.[17] As an important modulator of the innate immune system, IFN-α induces the rapid differentiation and activation of dendritic cells[18-20] and enhances the cytotoxicity, migration, cytokine production, and antibody-dependent cellular cytotoxicity (ADCC) of natural killer (NK) cells.[21,22]

The promise of IFN-α as a cancer therapeutic has been hindered primarily because of its short circulating half-life ($t_{1/2}$) and systemic toxicity. PEGylated forms of IFN-α2 display increased circulation time, which augments their biologic efficacy.[23,24] Fusion of IFN-α to a monoclonal antibody (mAb) can provide similar benefits as PEGylation, including reduced renal clearance, improved solubility and stability, and markedly increased circulating $t_{1/2}$. The immediate clinical benefit of this is less frequent and lower doses, allowing prolonged therapeutic concentrations. Targeting IFN-α to tumors using mAbs to a tumor-associated antigen can significantly increase its tumor accretion and retention while limiting its systemic concentration, thereby increasing the therapeutic index. Increased tumor concentrations of IFN-α can augment its direct antiproliferative, apoptotic, and antiangiogenic activity, as well as prime and focus an antitumor immune response. Indeed, studies in mice using syngeneic murine IFN-α–secreting transgenic tumors demonstrated an enhanced immune response elicited by a localized concentration of IFN-α.[25]

CD20 is an attractive candidate tumor-associated antigen for the therapy of B-cell lymphomas using a mAb-IFN-α conjugate (mAb-IFN-α). Anti-CD20 immunotherapy with rituximab is one of the most successful therapies against lymphoma with relatively low toxicity.[26] Because rituximab is a chimeric antibody that can show immunogenicity in some patient populations and has considerably long infusion times for the initial administration,[27] we chose the humanized mAb, veltuzumab (v-mab),[28] for CD20 targeting.

Combination therapies with rituximab and IFN-α currently under clinical evaluation have shown improved efficacy over rituximab alone.[29,30] These studies demonstrate both advantages of this combination and drawbacks associated with IFN-α. In addition to weekly infusions with rituximab, patients are typically administered IFN-α 3 times per week for months and have the flu-like symptoms common to IFN-α therapy, which limit the tolerable dose. An anti-CD20 mAb-IFN-α conjugate could allow the less frequent administration of a single agent at a lower dose, limit or eliminate side effects, and may result in far superior efficacy.

For this study, mAb-IFN-α immunocytokines comprising 4 IFN-α2b groups were prepared using the dock-and-lock (DNL) method,[31] which has been shown to generate stable and defined conjugates suitable for in vivo applications[32-38]; 20-2b, a CD20-targeting

Submitted June 19, 2009; accepted August 9, 2009. Prepublished online as *Blood* First Edition paper, August 26, 2009; DOI 10.1182/blood-2009-06-228890.

The online version of this article contains a data supplement.

The publication costs of this article were defrayed in part by page charge payment. Therefore, and solely to indicate this fact, this article is hereby marked "advertisement" in accordance with 18 USC section 1734.

mAb-IFN-α, was found to be a superior antilymphoma agent to either v-mab or a nontargeting mAb-IFN-α using in vitro proliferation, ex vivo lymphoma cell depletion, and in vivo therapy studies.

Methods

Antibodies and reagents

Humanized antibodies (provided by Immunomedics Inc) included v-mab (anti-CD20 IgG_1), epratuzumab (anti-CD22 IgG_1), and h734 [anti-In-DTPA (indium diethylene triamine pentaacetic acid) IgG_1]. PEGASYS (Peginterferon alph-2a, Hoffmann-La Roche) and PEG-Intron (Peginterferon alph-2b, Schering Corp) were used as controls for various studies.

mAb-IFN-α constructs

The 20-2b was produced by DNL via the combination of 2 DNL modules, C_H3-AD2-IgG-v-mab and IFN-α2b-DDD2, which were each expressed in Sp/ESF cells. Additional DNL-generated mAb-IFN-α constructs, of similar design as 20-2b (humanized IgG_1 plus 4 IFN-α2b) but with different targeting mAbs, were used as controls in several experiments (Table 1): 22-2b has C_H3-AD2-IgG-e-mab (epratuzumab) as its AD2 module, which is directed against CD22 and binds lymphoma; 734-2b has C_H3-AD2-IgG-h734 as its AD2 module, which is directed against the hapten, In-DTPA, and does not bind to any animal proteins or tissues; and R1-2b uses C_H3-AD2-IgG-hR1, which binds human insulin-like growth factor 1 receptor. Methods used in the production of the DNL modules and generation of 20-2b are provided as supplemental methods (available on the *Blood* website; see the Supplemental Materials link at the top of the online article).

Analytical methods

Protein concentrations of IFN-α constructs were measured using a commercial human IFN-α2 enzyme-linked immunosorbent assay (ELISA) kit following the manufacturer's suggested protocol (PBL Interferon Source) and confirmed by size-exclusion high-performance liquid chromatography (SE-HPLC) performed on a Beckman System Gold Model 116 with a Bio-Sil SEC 250 column (Bio-Rad) and 0.04 M phosphate-buffered saline (PBS), pH 6.8, 1 mM ethylenediaminetetraacetic acid as the mobile phase. Reducing and nonreducing sodium dodecyl sulfate–polyacrylamide gel electrophoresis analyses were performed using 4% to 20% gradient Tris-glycine gels (Cambrex Bio Science). All colorimetric (ELISA and in vitro proliferation), luminescence (reporter), and fluorometric (complement-dependent cytotoxicity [CDC] and ADCC) assays were quantified with an EnVision 2100 Multilabel Plate Reader (PerkinElmer Life and Analytical Sciences).

Cell binding

The 20-2b, v-mab, and h734 were labeled with phycoerythrin using a Zenon R-phycoerythrin human IgG labeling kit following the manufacturer's protocol (Invitrogen). Raji cells were incubated with the phycoerythrin mAbs (0.33 nM) at room temperature for 30 minutes, washed with 1% bovine serum albumin (BSA)-PBS, and binding was measured by flow cytometry on a Guava PCA using GuavaExpress software (Millipore).

IFN-α activity measurements

IFN-α2b specific activities were determined using the iLite Human Interferon Alpha Cell-Based Assay Kit following the manufacturer's suggested protocol (PBL Interferon Source). PEGASYS and mAb-IFN-α constructs were diluted to 10, 2.5, and 0.625 ng/mL in 1% BSA-PBS. PEG-Intron was diluted to 1, 0.25, and 0.0625 ng/mL. Each dilution was assayed in triplicate with overnight incubation with the supplied cells. Specific activities were extrapolated from a standard curve generated with the supplied standard. Antiviral activities were determined with an in vitro viral challenge assay using encephalomyocarditis virus on A549 cells by an independent analytical laboratory (PBL Interferon Source).

Table 1. mAb-IFN-α conjugates

	C_H3-AD2-IgG module	Binding specificity
20-2b	C_H3-AD2-IgG-v-mab	CD20
22-2b	C_H3-AD2-IgG-e-mab	CD22
734-2b	C_H3-AD2-IgG-h734	In-DTPA
1R-2b	C_H3-AD2-IgG-hR1	IGF-1R

In vitro proliferation

Daudi or Jeko-1 were plated at 5000 cells/well in 96-well plates and incubated at 37°C for 4 (Daudi) or 5 (Jeko-1) days in the presence of increasing concentrations of the indicated agents. Viable cell densities were determined using a CellTiter 96 Cell Proliferation Assay (Promega).

Ex vivo and in vivo methods

Blood specimens were collected under a protocol approved by the New England Institutional Review Board (Wellesley, MA), with donors giving informed consent in accordance with the Declaration of Helsinki. All animal studies were approved by the Center for Molecular Medicine and Immunology Institutional Animal Care and Use Committee, and performed in accordance with the Association for Assessment and Accreditation of Laboratory Animal Care, U.S. Department of Agriculture, and Department of Health and Human Services regulations. In vitro ADCC and CDC activity was assayed as described previously.[36]

Stability in human serum and whole blood

The 20-2b was diluted to 5 μg/mL in freshly isolated heparinized human blood or serum and incubated at 37°C and 5% CO_2 for up to 10 days (for serum). The serum concentration of intact 20-2b at each time point was measured using a bispecific sandwich ELISA. Microtiter plates were coated at 5 μg/mL with WR2 (Immunomedics), a rat anti-idiotype mAb to v-mab, and blocked with 1% BSA. Serum dilutions were incubated for 1 hour to allow capture of 20-2b via binding of the v-mab moiety. The 20-2b was detected with rabbit anti–human IFN-α2 polyclonal antibody (Millipore) and quantified with peroxidase-conjugated goat anti–rabbit IgG (Jackson ImmunoResearch) and o-phenylenediamine dihydrochloride.

Pharmacokinetics in mice

Groups of 4 male Swiss-Webster mice were injected subcutaneously with 100 pmol of 20-2b (25 μg), PEGASYS (6 μg), or PEG-Intron (3 μg). Animals were bled at 0.5, 2, 8, 24, 48, 72, and 96 hours. Serum concentrations of IFN-α2 were measured using a commercial human IFN-α2 ELISA kit following the manufacturer's suggested protocol (PBL Interferon Source). For pharmacokinetics analysis, blood concentrations of each reagent as determined from the percentage injected dose values were plotted and analyzed using the WinNonLin Pk software package (Version 5.1; Pharsight Corp).

Ex vivo depletion of Daudi and Ramos lymphoma cells from whole blood

The effects of 20-2b on non-Hodgkin lymphoma (NHL) cells as well as peripheral blood lymphocytes in whole human blood from healthy volunteers were evaluated ex vivo using flow cytometry and compared with those of v-mab, 734-2b, or a combination of v-mab and 734-2b. Daudi or Ramos cells (5×10^4) were mixed with heparinized whole blood (150 μL) and incubated with test mAbs at 0.01, 0.1, or 1 nM for 2 days at 37°C and 5% CO_2. Cells were stained with fluorescein isothiocyanate–labeled anti-CD3, anti-CD19, or mouse IgG_1 isotype control (BD Biosciences). After lysis of erythrocytes, cells were analyzed using a FACSCalibur (BD Biosciences) with CellQuest software. Both Daudi and Ramos cells are $CD19^+$ and in the monocyte gate. The normal B and T cells are $CD19^+$ and $CD3^+$ cells, respectively, in the lymphocyte gate. Student *t* test was used to evaluate statistical significance ($P < .05$).

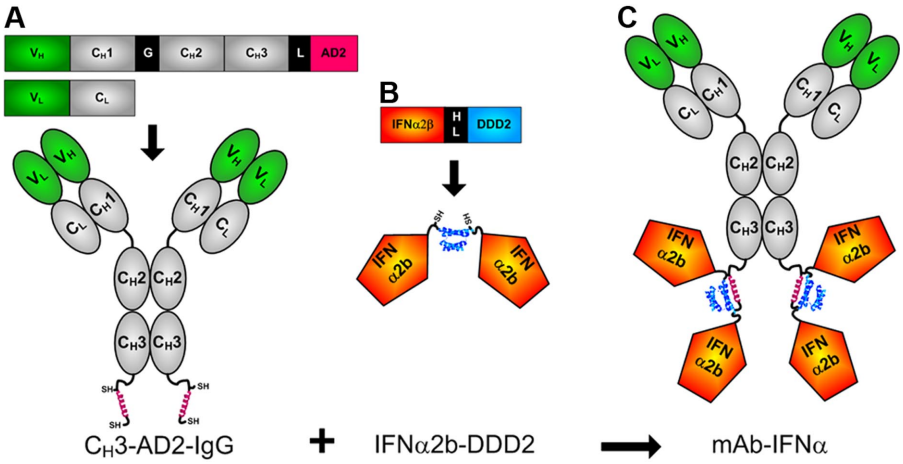

Figure 1. Schematic diagrams of 20-2b and its constituent DNL modules. Expression cassettes and structures of (A) C_H3-AD2-IgG, (B) IFN-α2b-DDD2, and (C) 20-2b. Blue helix represents DDD2; red helix, AD2; SH indicates sulfhydryl groups of engineered cysteines; V, variable (green); C, constant (gray); G, hinge; L, linker (GSGGGGSGG); HL, 6-His/linker, HL (EKSHHHHHHGSGGGGSGGG). C_H3-AD2-IgG-v-mab, C_H3-AD2-IgG-e-mab, C_H3-AD2-IgG-734, and C_H3-AD2-IgG-hR1 modules (A) were used to generate 20-2b, 22-2b, 734-2b, and 1R-2b, respectively.

In vivo efficacy in mice

Female C.B.17 homozygous severe combined immunodeficiency (SCID) mice (Taconic Farms) were inoculated intravenously with 1.5×10^7 Daudi, 2.5×10^6 Raji, or 5×10^6 NAMALWA cells on day 0. Treatments were administered by subcutaneous injection. Saline was used as a control treatment. Animals, monitored daily, were humanely killed when hind-limb paralysis developed or if they became otherwise moribund. In addition, mice were killed if they lost more than 20% of initial body weight. Survival curves were analyzed using Kaplan-Meier plots (log-rank analysis), using the Prism (Version 4.03) software package (GraphPad Software). Some outliers determined by critical Z test were censored from analyses.

Results

The DNL method was adopted to site-specifically conjugate 4 IFN-α2b groups to the carboxyl terminus of the C_H3 domains of humanized mAbs (Figure 1). The prototype conjugate, called 20-2b, which comprises v-mab (anti-CD20) for targeting IFN-α2b to B-cell lymphoma, was produced by DNL by combination of 2 DNL modules, C_H3-AD2-IgG-v-mab (Figure 1A) and IFN-α2b-DDD2 (Figure 1B). Production, purification, and characterization of the modules and 20-2b are provided as supplemental results. The size and purity of 20-2b were demonstrated by SE-HPLC and sodium dodecyl sulfate–polyacrylamide gel electrophoresis; its ability to bind cellular CD20 (similar to v-mab) was shown with flow cytometry (supplemental Figure 1).

Biologic activity

We compared the in vitro IFN-α biologic activity of 20-2b with that of commercial pegylated IFN-α2 agents, PEGASYS and PEG-Intron, using cell-based reporter, viral protection, and lymphoma proliferation assays (Figure 2). Specific activities were determined using a cell-based kit, which uses a transgenic human promonocyte cell line carrying a reporter gene fused to an interferon-stimulated response element (Figure 2A). The specific activity of 20-2b (5300 IU/pmol) was greater than both PEGASYS (170 IU/pmol) and PEG-Intron (3400 IU/pmol). The 734-2b and 1R-2b were produced similarly to 20-2b and exhibited similar specific activities, demonstrating the consistency of the DNL method for generating such structures.

Comparison of mAb-IFN-α, PEGASYS, and PEG-Intron in an in vitro viral protection assay demonstrated that mAb-IFN-α retains IFN-α2b antiviral activity with specific activities similar to PEG-Intron and 10-fold greater than PEGASYS (Figure 2B).

IFN-α2b can have a direct antiproliferative or cytotoxic effect on some tumor lines. We measured the activity of 20-2b in an in

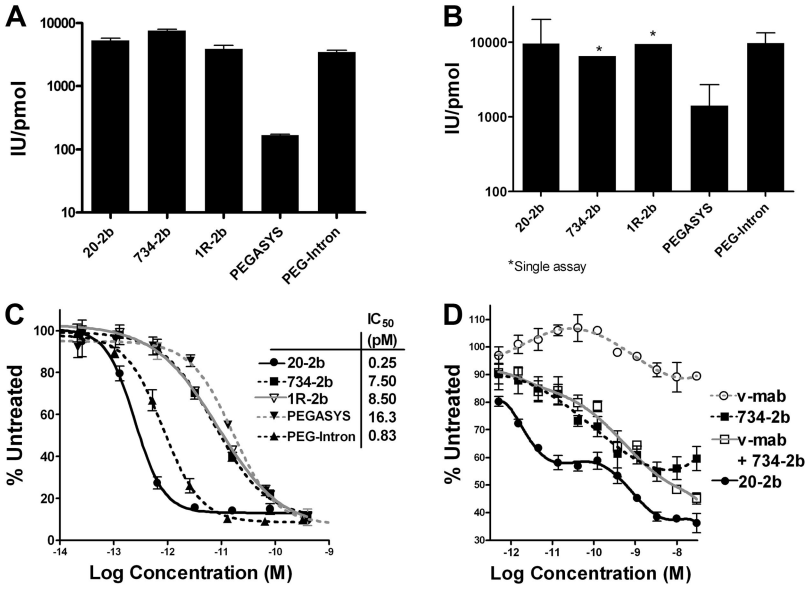

Figure 2. In vitro IFN-α activity. Specific activities (IU/pmol) measured using (A) cell-based reporter gene assay and (B) in vitro viral protection assay with EMC virus and A549 cells. The activity of known concentrations of each test article was extrapolated from a rhIFN-α2b standard curve. In vitro lymphoma proliferation assays were performed using (C) Daudi and (D) Jeko-1 cells. Cultures were grown in the presence of increasing concentrations of 20-2b (●), 734-2b (■), v-mab (○), v-mab plus 734-2b (□), PEGASYS (▼), PEG-Intron (▲), or 1R-2b (▽), and the relative viable cell densities were measured with MTS. The percentage of the signal obtained from untreated cells was plotted versus the log of the molar concentration. Dose-response curves and EC_{50} values were generated using Prism software. Error bars represent SD.

vitro proliferation assay with a Burkitt lymphoma cell line (Daudi) that is highly sensitive to IFN-α (Figure 2C). Each of the IFN-α2 agents efficiently inhibits (> 90%) Daudi in vitro with high potency (EC_{50} = 4-10 pM); however, 20-2b (EC_{50} = 0.25 pM) is approximately 30-fold more potent than the nontargeting mAb-IFN-α constructs (734-2b and 1R-2b). We have shown that v-mab has antiproliferative activity in vitro on many lymphoma cell lines, including Daudi,[36] at considerably greater concentrations (EC_{50} > 10 nM) than used here. The in vitro activity of 20-2b was also assessed using Jeko-1, which is a mantle cell lymphoma line that has lower sensitivity to both IFN-α and anti-CD20 (Figure 2D). Jeko-1 is only modestly sensitive to v-mab, having 10% maximal inhibition (I_{max}) with an EC_{50} near 1 nM. As shown with 734-2b, Jeko-1 (I_{max} = 43%; EC_{50} = 23 pM) is less responsive to IFN-α2b than Daudi (I_{max} = 90%; EC_{50} = 7.5 pM). Compared with 734-2b, 20-2b inhibited Jeko-1 to a greater extent (I_{max} = 65%) and exhibited a biphasic dose-response curve. At < 10 pM, a low-concentration response attributed to IFN-α2b activity is observed, which plateaus at I_{max} = 43%, similar to 734-2b. A high-concentration response was evident above 100 pM, where I_{max} reached 65%. The low-concentration IFN-α2b response of 20-2b (EC_{50} = 0.97 pM) is 25-fold more potent than 734-2b, similar to the results with Daudi. The dose-response curve for a combination of v-mab and 734-2b (v-mab + 734-2b) was largely similar to 734-2b alone, except at more than 1 nM, where inhibition increased for the former but not the latter. These results suggest that mAb targeting is responsible for the lower EC_{50} of 20-2b, but its greater I_{max} is apparently the result of the additive activity of IFN-α2b and CD20 signaling. The effect of CD20 signaling is only evident at the high concentration response for 20-2b (EC_{50} = 0.85 nM), which parallels the response to v-mab (EC_{50} = 1.5 nM). A biphasic dose-response curve is not obvious for v-mab plus 734-2b because the 2 responses overlap; however, an additive effect is evident at more than 1 nM concentrations. The I_{max} of 20-2b (65%) is significantly ($P < .001$) greater than the added responses of IFN-α2b (I_{max} = 43%) and v-mab (I_{max} = 10%).

Effector functions

IFN-α can potentiate ADCC, which is a fundamental mechanism of action (MOA) for anti-CD20 immunotherapy, by activating NK cells and macrophages. We compared ADCC of 20-2b and v-mab with 2 NHL cell lines using peripheral blood mononuclear cells (PBMCs) as effector cells. Replicate assays using PBMCs from multiple donors consistently demonstrated that 20-2b has enhanced ADCC compared with v-mab, as shown for both Daudi and Raji cells (Figure 3A). This effect was also shown with 22-2b, a mAb-IFN-α comprising the anti-CD22 mAb, epratuzumab, which shows modest ADCC.[39]

CDC is thought to be an important MOA for type I anti-CD20 mAbs (including v-mab and rituximab); however, this function is lacking in the type II mAbs, represented by tositumomab,[40] which nonetheless has antilymphoma activity. Unlike v-mab, 20-2b does not show CDC activity in vitro (Figure 3B). These results are consistent with those for other DNL structures based on the C_H3-AD2-IgG-v-mab module, in which complement fixation is apparently impaired, perhaps by steric hindrance.[36]

Stability in human blood

The 20-2b was stable in human sera (≥ 10 days) or whole blood (≥ 6 days) at 37°C (supplemental Figure 2A). The concentration of intact 20-2b was determined using a bispecific sandwich ELISA, in which 20-2b is captured using an anti-idiotype mAb to v-mab and detected with anti-IFN-α2.

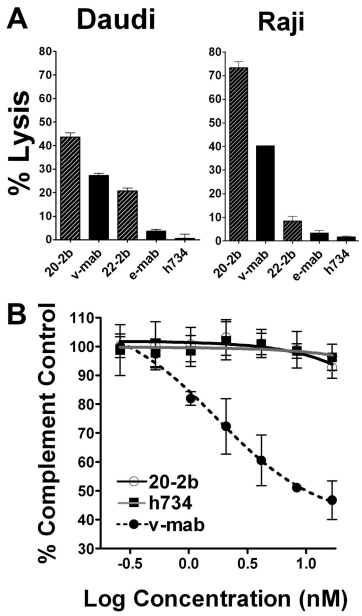

Figure 3. Effector functions. (A) ADCC. Daudi or Raji cells were incubated with 20-2b, 22-2b, v-mab, e-mab, or h734 at 5 μg/mL in the presence of freshly isolated PBMCs for 4 hours before quantification of cell lysis. Effector/target ratio = 50:1. (B) CDC. Daudi cells were incubated with serial dilutions of 20-2b (○), h734 (■), or v-mab (●) in the presence of human complement. The percentage complement control (number of viable cells in the test sample compared with cells treated with complement only) was plotted versus the log of the namomolar concentration. Error bars represent SD.

Pharmacokinetics in mice

As a therapeutic agent, recombinant IFN-α is markedly limited by its very rapid rate of clearance. We determined the pharmacokinetic parameters for recombinant IFN-α2b in mice, finding a mean residence time of only 0.7 hours (data not shown). Commercial IFN-α2 agents have been developed to extend blood clearance by either PEGylation (PEG-Intron and PEGASYS) or fusion to human serum albumin (Albuferon). Because of their substantially longer circulating serum $t_{1/2}$, these agents require less frequent dosing, show improved clinical efficacy, and essentially have replaced the use of recombinant IFN-α2b for the treatment of hepatitis and some cancers. Comparative pharmacokinetic analysis in mice (supplemental Figure 2B) gave a significantly longer $t_{1/2}$ for 20-2b (23.4 hours) compared with either PEGASYS (14.9 hours) or PEG-Intron (9.3 hours; $P < .019$). This increased $t_{1/2}$ resulted in a significantly ($P < .002$) longer mean residence time for 20-2b (47.6 hours) than either PEGASYS (33.5 hours) or PEG-Intron (17.1 hours).

Ex vivo depletion of lymphoma from whole human blood

We compared the abilities of 20-2b, v-mab, 734-2b (control), or v-mab plus 734-2b to eliminate lymphoma or normal B cells from whole blood in an ex vivo setting (Figure 4). The therapeutic efficacy of naked anti-CD20 mAbs is thought to be achieved via 3 MOA: signaling-induced apoptosis or growth arrest, ADCC, and CDC.[41] In this assay, v-mab can use all 3 MOA, whereas, based on the in vitro findings, 20-2b can potentially take advantage of signaling and enhanced ADCC, but not CDC. In this short-term model, the IFN-α2b groups of 20-2b and 734-2b can act directly on tumor cells, augment the ADCC activity of v-mab, and possibly

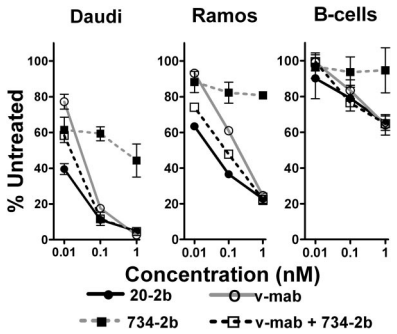

Figure 4. Enhanced depletion of NHL cells from whole blood. Fresh heparinized human blood was mixed with either Daudi or Ramos and incubated with 20-2b (●), v-mab (○), 734-2b (■), or v-mab plus 734-2b (□) at 0.01, 0.1, or 1 nM for 2 days. The effect of the indicated treatments on lymphoma and peripheral blood lymphocytes was evaluated using flow cytometry. Error bars represent SD.

have some immunostimulatory effects. However, the full spectrum of IFN-α–mediated activation of the innate and adaptive immune systems that might occur in vivo is not realized in this 2-day ex vivo assay.

At 0.01 nM, 20-2b depleted Daudi cells (60.5%) significantly more than v-mab (22.8%), 734-2b (38.6%), or v-mab plus 734-2b (41.7%). At 0.1 nM, 20-2b and v-mab plus 734-2b depleted Daudi to a similar extent (88.9%), which was more than for v-mab (82.4%) or 734-2b (40.7%). At 1 nM, each agent depleted Daudi more than 95%, except for 734-2b (55.7%). All indicated differences were statistically significant ($P < .01$).

Ramos is less sensitive than Daudi to both IFN-α2b and v-mab. The effect of 734-2b was only moderate, resulting in less than 20% depletion of Ramos at each concentration. At both 0.01 and 0.1 nM, 20-2b depleted Ramos more than v-mab plus 734-2b, which in turn eliminated more cells than v-mab. At 1 nM, all treatments besides 734-2b resulted in similar Ramos depletion (75%). All indicated differences were statistically significant ($P < .02$).

As demonstrated with 734-2b, IFN-α2b does not deplete normal B cells in this assay. At these low concentrations, 20-2b, v-mab, and v-mab plus 734-2b each show similar dose-responsive depletion of B cells, which is markedly less than the depletion of either Daudi or Ramos. None of the treatments resulted in significant depletion of T cells (data not shown).

In vivo efficacy in SCID mice

A major limitation of the mouse model is the very low sensitivity of murine cells to human IFN-α2b, prohibiting our evaluation of the overall therapeutic advantage of 20-2b that might be achieved in humans, which can involve the enhancement of both innate and adaptive immunity. With these limitations in mind, we studied the antilymphoma in vivo efficacy of 20-2b against disseminated Burkitt lymphoma models in SCID mice. We initially tested a highly sensitive early Daudi model, with groups administered a single low dose of 20-2b, v-mab, or 734-2b 1 day after tumor inoculation (Figure 5A). A single dose of v-mab but not 734-2b at 0.7 pmol (170 ng) resulted in a modest (34 days), yet significant ($P < .001$), improvement in median survival time (MST) compared with saline (27 days). However, a single dose of 0.7 pmol (170 ng) of 20-2b improved the MST by more than 100 days over both saline control and v-mab groups ($P < .001$). The study was terminated after 19 weeks, at which time the 7 long-term survivors (LTSs) in the 0.7 pmol 20-2b treatment group were necropsied with no visible evidence of disease found (cured). Remarkably, even the lowest dose of 0.07 pmol (17 ng) of 20-2b more than doubled the MST.

Next, we assessed the efficacy of 20-2b in a more challenging advanced Daudi model, in which mice were allowed to develop a substantially greater tumor burden before treatment (Figure 5B). Seven days after tumor inoculation, groups were administered a single dose (0.7, 7.0, or 70 pmol) of 20-2b, v-mab, 734-2b, or PEGASYS. The MST for the saline control mice was 21 days. The highest dose (70 pmol) of PEGASYS (4.25 μg) or 734-2b (17 μg) doubled the MST (42 days; $P < .001$). Treatment with 20-2b at a 100-fold lower dose (0.7 pmol; 170 ng) produced similar results (38.5 days) as the highest dose (70 pmol) of either PEGASYS or 734-2b. Treatment with 20-2b at a 10-fold lower dose (7 pmol; 1.7 μg) resulted in significantly improved survival (80.5 days, 20% LTS) over treatment with 70 pmol of PEGASYS or 734-2b ($P < .002$). At the highest dose tested (70 pmol; 17 μg), 20-2b improved the MST to more than 105 days with 100% LTSs. We have demonstrated previously with the early tumor model that v-mab can increase survival of Daudi-bearing mice at relatively low doses (3.5 pmol; 0.5 μg), whereas higher doses result in long-term survival. However, in this advanced tumor model, a single dose of 70 pmol (10 μg) of v-mab had only a modest, although significant, effect on survival (MST = 24 days, $P < .001$).

We subsequently assayed 20-2b in more challenging models, which are less sensitive than Daudi to direct inhibition by IFN-α and less responsive to immunotherapy with v-mab. Compared with Daudi, Raji has a similar CD20 antigen density,[42] is less responsive to v-mab,[43] and is approximately 1000-fold less sensitive to the direct action of IFN-α2b (supplemental Figure 3). The efficacy of 20-2b was studied in an advanced Raji model with therapy beginning 5 days after tumor inoculation (Figure 6A). Groups were administered a total of 6 injections (250 pmol each) over 2 weeks. The 734-2b did not improve survival over saline (MST = 16 days), consistent with the insensitivity of Raji to IFN-α. V-mab improved survival over saline (MST = 26 days, $P < .001$). The 20-2b was superior to all other treatments (MST = 33 days, $P < .001$).

Finally, we investigated the efficacy of 20-2b with NAMALWA (Figure 6B), a human lymphoma that has low sensitivity to the

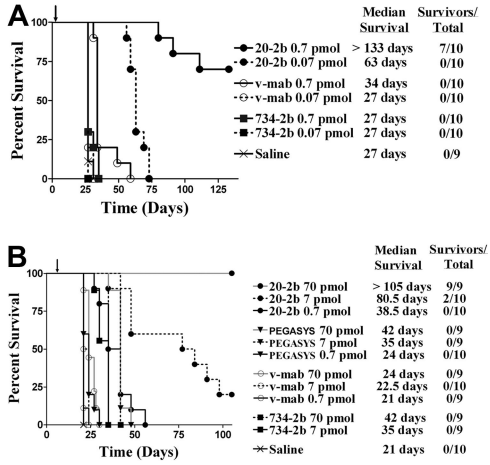

Figure 5. Survival curves showing therapeutic efficacy of 20-2b in a disseminated Burkitt lymphoma (Daudi) xenograft model. Female C.B.17 SCID mice were administered Daudi cells intravenously on day 0. Treatments consisted of 20-2b (●), 734-2b (■), v-mab (○), PEGASYS (▼), or saline (X) given as a single subcutaneous dose. Days of treatment are indicated with arrows. Survival curves were analyzed using Prism software. (A) Early Daudi model. Groups of 10 mice were given a single dose of 0.7 pmol (solid line) or 0.07 pmol (dashed line) on day 1. (B) Advanced Daudi model. Groups of 10 mice were given a single dose of 0.7 pmol (solid line), 7 pmol (dashed line), or 70 pmol (gray line) on day 7.

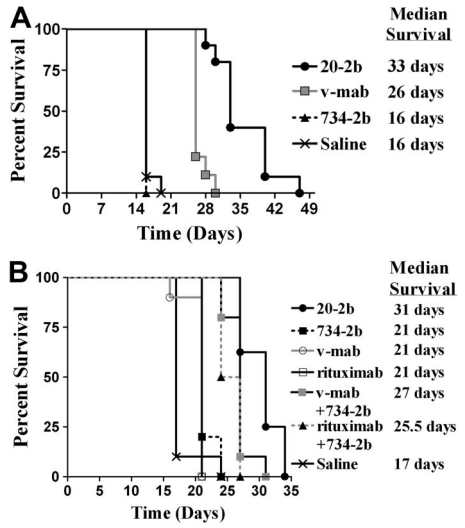

Figure 6. Survival curves showing therapeutic efficacy of 20-2b in disseminated Burkitt lymphoma (Raji and NAMALWA) xenograft models. Female C.B. 17 SCID mice were administered NHL cells intravenously on day 0. (A) Advanced Raji model. Groups of 10 received 250-pmol doses on days 5, 7, 9, 12, 14, and 16. Treatments consisted of 20-2b (●), 734-2b (■), v-mab (○), or saline (X) given as subcutaneous doses. (B) Early NAMALWA model. Groups of 10 received 250-pmol doses on days 1, 3, 5, 8, 10, and 12. Treatments consisted of 20-2b (●), 734-2b (■), v-mab (○), rituximab (□), v-mab plus 734-2b (■), rituximab plus 734-2b (▲), or saline (X) given as subcutaneous doses. Survival curves were analyzed using Prism software.

direct action of IFN-α, approximately 25-fold lower CD20 antigen density compared with Daudi or Raji, and is considered to be resistant to anti-CD20 immunotherapy.[42] Groups were administered a total of 6 doses (250 pmol each) of 20-2b, 734-2b, v-mab, or rituximab. Additional groups were administered 6 doses of a combination of v-mab plus 734-2b or rituximab plus 734-2b (250 pmol of each agent/dose). The group treated with saline had an MST of 17 days. Treatment with 734-2b, v-mab, or rituximab as single agents resulted in similarly modest, although significant, increased survival (MST = 21 days, $P < .024$). The combination of v-mab plus 734-2b (MST = 27 days) or rituximab plus 734-2b (MST = 25.5 days) were each superior to treatment with any single agent ($P < .001$). The 20-2b (MST = 31 days) was superior to all other treatments ($P < .013$).

Discussion

We developed the first tetrameric immunocytokine, designated 20-2b, which comprises 4 IFN-α2b groups site-specifically tethered to a humanized anti-CD20 mAb, and evaluated its potential for B-cell lymphoma therapy. The results demonstrate that targeting makes this immunocytokine more potent and effective than either agent alone or in combination. mAb targeting of IFN-α to tumors may allow a less frequent dosing schedule of a single agent, reduce or eliminate side effects associated with IFN therapy, and result in profoundly enhanced efficacy. In addition, targeted IFN-α can induce an acute tumor-directed immune response and possibly evoke immune memory via pleiotropic stimulation of innate and adaptive immunity.[44] Other groups have produced mAb-IFN-α made by chemical conjugation that revealed some of the potential clinical benefits of such constructs.[45,46] A recombinant mAb-IFN-α comprising murine IFN-α and an anti-HER2/neu mAb exhibited potent inhibition of a transgenic (HER2/neu) murine B-cell lymphoma in immunocompetent mice and was also capable of inducing a protective adaptive immune response with immunologic memory.[47] Based on an extensive literature, it is reasonable to expect that therapy with 20-2b will stimulate localized recruitment and activation of several immune cells, including NK, T4, T8, and dendritic cells, resulting in enhanced cytotoxicity and ADCC, and may potentially induce tumor-directed immunologic memory. However, in this study, we were limited by the lack of an appropriate animal model, in which the host is reasonably responsive to human IFN-α2b and also receptive of human lymphoma xenografts, and would therefore allow the evaluation of all of the potential benefits of 20-2b therapy. Murine cells are considerably less sensitive (~ 4 logs) than human cells to human IFN-α2b.[48,49] Therefore, very little, if any, of the antilymphoma activity of 20-2b in the mouse model can be attributed to IFN-α2b activation of the mouse immune response; rather, killing is primarily the result of the direct action of IFN-α2b on the lymphoma cells. We have shown that 20-2b has augmented ADCC, which may be the most important MOA of anti-CD20 immunotherapy.[36] However, because human IFN-α2b is only a very weak stimulator of the murine host's immune effector cells, an IFN-α–enhanced ADCC is probably not realized as it might be in humans. Even with these limitations, the in vivo results demonstrate that 20-2b can be a highly effective antilymphoma agent, exhibiting more than 100 times the potency of v-mab or a nontargeting mAb-IFN-α in the IFN-α–sensitive Daudi model. Even with lymphoma models that are relatively insensitive to the direct action of IFN-α (Raji/NAMALWA) or are resistant to anti-CD20 immunotherapy (NAMALWA), 20-2b showed superior efficacy to either v-mab or nontargeted mAb-IFN-α. Fusion of IFN-α2b to v-mab increases its in vivo potency by extending circulation times and enabling tumor targeting. The therapeutic significance of pharmacokinetics was demonstrated in the Daudi model, where the slower-clearing PEGASYS was superior to the faster-clearing PEG-Intron, which has a higher specific activity (data not shown). The 20-2b was considerably more potent than either PEGASYS or 734-2b, suggesting that lymphoma targeting via the anti-CD20 mAb is critical to its superior potency and efficacy. This was substantiated in the NAMALWA model, where 20-2b, as a single agent, was superior to a combination of v-mab (or rituximab) plus nontargeted mAb-IFN-α (734-2b). The impact of targeting was evident even in the in vitro assays, which was surprising because the mAbs, effector, and target cells are all confined throughout the experiments. The 20-2b inhibited lymphoma proliferation in vitro at a 25-fold lower concentration compared with v-mab plus 734-2b. Even without CDC, 20-2b was more effective at depleting lymphoma cells from blood than v-mab plus 734-2b. The enhanced in vitro efficacy of 20-2b compared with the combination may be solely the result of an increased local concentration of IFN-α resulting from tumor targeting. Alternatively, the binding of CD20 may prevent the internalization/down-regulation of the type I IFN receptors, resulting in a more prolonged and effective IFN-α–induced signal.

The combination of v-mab and the control mAb-IFN-α, 734-2b, although not as effective as 20-2b, was nonetheless superior to either v-mab or control mAb-IFN-α alone in therapy studies with NAMALWA, ex vivo depletion of Daudi and Ramos from whole blood, and in vitro proliferation inhibition of Jeko-1. It is unclear whether the improved efficacy of this combination, which in vivo (and ex vivo) can potentially kill lymphoma cells using all 3 MOAs of anti-CD20 immunotherapy in addition to the direct actions of IFN-α, is a result of IFN-α–enhanced anti-CD20 activity, anti-CD20–enhanced IFN-α activity, or merely the additive actions of the 2 agents. In the ex vivo experiments using human blood, the

ADCC activity of v-mab as part of 20-2b or when combined with 734-2b may be augmented by IFN-α, yet ADCC is not functional in the in vitro proliferation assays and not expected to be modulated by human IFN-α in the mouse model, suggesting additional mechanisms.

We made every effort in the design of 20-2b to limit its potential immunogenicity. Human IFN-α2b and the fully humanized v-mab were fused to a DDD2 and AD2, respectively, which each consists of the smallest functional peptides derived from human protein sequences but possesses additional, unnatural cysteine residues. Clinical studies will be needed to evaluate immunogenicity. Having 4 IFN-α2b groups may lead to an increased binding avidity to type I receptors on normal cells and therefore may affect its overall biodistribution and pharmacodynamics. It could be argued that this potentially enhanced binding avidity could lead to increased IFN-related toxicity via systemic activation of immune cells in patients. However, both the cell-based reporter gene and viral protection assays demonstrated that 20-2b and PEG-Intron have similar specific activities, which are considerably lower than that of recombinant IFN-α2b, making it less probable that increased toxicity will be experienced compared with current IFN-α therapy regimens, especially if 20-2b can be given at lower doses. Biodistibution, pharmacodynamics, and toxicity must be evaluated in primates before clinical trials. The findings in this study indicate that 20-2b may be a highly effective lymphoma therapeutic. We are now developing other mAb-IFN-α constructs for the therapy of a variety of cancers.

Acknowledgments

The authors thank Diane Nordstrom, Diana Pilas, Eric Chan, Roberto Arrojo, Preeti Trisal, Anju Nair, and John Kopinski for excellent technical assistance.

This work was supported in part by the National Cancer Institute (P01-CA103985) of the National Institutes of Health (D.M.G.).

Authorship

Contribution: E.A.R., D.M.G., and C.-H.C. designed research, analyzed data, and wrote the paper; and T.M.C. and R.S. performed research, collected and analyzed data, and revised the paper.

Conflict-of-interest disclosure: All of the authors, except R.S., have employment, stock, and/or stock options with Immunomedics Inc.

Correspondence: Edmund A. Rossi, Immunomedics Inc, 300 American Rd, Morris Plains, NJ 07950; e-mail: erossi@immunomedics.com; and David M. Goldenberg, Garden State Cancer Center, Center for Molecular Medicine and Immunology, 520 Belleville Ave, Belleville, NJ 07910; e-mail: dmg.gscancer@worldnet.att.net.

References

1. Ferrantini M, Giovarelli M, Modesti A, et al. IFN-alpha 1 gene expression into a metastatic murine adenocarcinoma (TS/A) results in CD8+ T cell-mediated tumor rejection and development of antitumor immunity: comparative studies with IFN-gamma-producing TS/A cells. *J Immunol.* 1994; 153(10):4604-4615.
2. Gresser I, Coppey J, Bourali C. [Inhibiting action of crude interferon on lymphoid leukemia in AKR mice]. *C R Acad Sci Hebd Seances Acad Sci D.* 1968;267(22):1900-1902.
3. Gresser I, Maury C, Brouty-Boye D. Mechanism of the antitumour effect of interferon in mice. *Nature.* 1972;239(5368):167-168.
4. Gutterman JU, Blumenschein GR, Alexanian R, et al. Leukocyte interferon-induced tumor regression in human metastatic breast cancer, multiple myeloma, and malignant lymphoma. *Ann Intern Med.* 1980;93(3):399-406.
5. Gutterman JU. Cytokine therapeutics: lessons from interferon alpha. *Proc Natl Acad Sci U S A.* 1994;91(4):1198-1205.
6. Matarrese P, Di Biase L, Santodonato L, et al. Type I interferon gene transfer sensitizes melanoma cells to apoptosis via a target activity on mitochondrial function. *Am J Pathol.* 2002;160(4): 1507-1520.
7. Mecchia M, Matarrese P, Malorni W, et al. Type I consensus interferon (CIFN) gene transfer into human melanoma cells up-regulates p53 and enhances cisplatin-induced apoptosis: implications for new therapeutic strategies with IFN-alpha. *Gene Ther.* 2000;7(2):167-179.
8. Sabaawy HM, Ikehara S, Adachi Y, et al. Enhancement of 5-fluorouracil cytotoxicity on human colon cancer cells by retrovirus-mediated interferon-alpha gene transfer. *Int J Oncol.* 1999; 14(6):1143-1151.
9. Takaoka A, Hayakawa S, Yanai H, et al. Integration of interferon-alpha/beta signalling to p53 responses in tumour suppression and antiviral defence. *Nature.* 2003;424(6948):516-523.
10. Grimley PM, Fang H, Rui H, et al. Prolonged STAT1 activation related to the growth arrest of malignant lymphoma cells by interferon-alpha. *Blood.* 1998;91(8):3017-3027.
11. Sidky YA, Borden EC. Inhibition of angiogenesis by interferons: effects on tumor- and lymphocyte-induced vascular responses. *Cancer Res.* 1987; 47(19):5155-5161.
12. Belardelli F, Gresser I. The neglected role of type I interferon in the T-cell response: implications for its clinical use. *Immunol Today.* 1996;17(8):369-372.
13. Raefsky EL, Platanias LC, Zoumbos NC, Young NS. Studies of interferon as a regulator of hematopoietic cell proliferation. *J Immunol.* 1985; 135(4):2507-2512.
14. Luft T, Pang KC, Thomas E, et al. Type I IFNs enhance the terminal differentiation of dendritic cells. *J Immunol.* 1998;161(4):1947-1953.
15. Carrero JA, Calderon B, Unanue ER. Lymphocytes are detrimental during the early innate immune response against Listeria monocytogenes. *J Exp Med.* 2006;203(4):933-940.
16. Pilling D, Akbar AN, Girdlestone J, et al. Interferon-beta mediates stromal cell rescue of T cells from apoptosis. *Eur J Immunol.* 1999;29(3):1041-1050.
17. Le Bon A, Schiavoni G, D'Agostino G, Gresser I, Belardelli F, Tough DF. Type i interferons potently enhance humoral immunity and can promote isotype switching by stimulating dendritic cells in vivo. *Immunity.* 2001;14(4):461-470.
18. Belardelli F, Ferrantini M, Parmiani G, Schlom J, Garaci E. International meeting on cancer vaccines: how can we enhance efficacy of therapeutic vaccines? *Cancer Res.* 2004;64(18):6827-6830.
19. Paquette RL, Hsu NC, Kiertscher SM, et al. Interferon-alpha and granulocyte-macrophage colony-stimulating factor differentiate peripheral blood monocytes into potent antigen-presenting cells. *J Leukoc Biol.* 1998;64(3):358-367.
20. Santini SM, Lapenta C, Logozzi M, et al. Type I interferon as a powerful adjuvant for monocyte-derived dendritic cell development and activity in vitro and in Hu-PBL-SCID mice. *J Exp Med.* 2000;191(10):1777-1788.
21. Biron CA, Nguyen KB, Pien GC, Cousens LP, Salazar-Mather TP. Natural killer cells in antiviral defense: function and regulation by innate cytokines. *Annu Rev Immunol.* 1999;17:189-220.
22. Brunda MJ, Rosenbaum D. Modulation of murine natural killer cell activity in vitro and in vivo by recombinant human interferons. *Cancer Res.* 1984; 44(2):597-601.
23. Harris JM, Chess RB. Effect of pegylation on pharmaceuticals. *Nat Rev Drug Discov.* 2003; 2(3):214-221.
24. Osborn BL, Olsen HS, Nardelli B, et al. Pharmacokinetic and pharmacodynamic studies of a human serum albumin-interferon-alpha fusion protein in cynomolgus monkeys. *J Pharmacol Exp Ther.* 2002;303(2):540-548.
25. Ferrantini M, Capone I, Belardelli F. Interferon-alpha and cancer: mechanisms of action and new perspectives of clinical use. *Biochimie.* 2007;89(6):884-893.
26. McLaughlin P, Grillo-Lopez AJ, Link BK, et al. Rituximab chimeric anti-CD20 monoclonal antibody therapy for relapsed indolent lymphoma: half of patients respond to a four-dose treatment program. *J Clin Oncol.* 1998;16(8):2825-2833.
27. Cheson BD, Leonard JP. Monoclonal antibody therapy for B-cell non-Hodgkin's lymphoma. *N Engl J Med.* 2008;359(6):613-626.
28. Stein R, Qu Z, Chen S, et al. Characterization of a new humanized anti-CD20 monoclonal antibody, IMMU-106, and its use in combination with the humanized anti-CD22 antibody, epratuzumab, for the therapy of non-Hodgkin's lymphoma. *Clin Cancer Res.* 2004;10(8):2868-2878.
29. Kimby E, Jurlander J, Geisler C, et al. Long-term molecular remissions in patients with indolent lymphoma treated with rituximab as a single agent or in combination with interferon alpha-2a:

a randomized phase II study from the Nordic Lymphoma Group. *Leuk Lymphoma.* 2008;49(1): 102-112.

30. Salles G, Mounier N, de Guibert S, et al. Rituximab combined with chemotherapy and interferon in follicular lymphoma patients: results of the GELA-GOELAMS FL2000 study. *Blood.* 2008; 112(13):4824-4831.
31. Chang CH, Rossi EA, Goldenberg DM. The dock and lock method: a novel platform technology for building multivalent, multifunctional structures of defined composition with retained bioactivity. *Clin Cancer Res.* 2007;13(18):5586S-5591S.
32. Gold DV, Goldenberg DM, Karacay H, et al. A novel bispecific, trivalent antibody construct for targeting pancreatic carcinoma. *Cancer Res.* 2008;68(12):4819-4826.
33. Goldenberg DM, Rossi EA, Sharkey RM, McBride WJ, Chang CH. Multifunctional antibodies by the Dock-and-Lock method for improved cancer imaging and therapy by pretargeting. *J Nucl Med.* 2008;49(1):158-163.
34. McBride WJ, Zanzonico P, Sharkey RM, et al. Bispecific antibody pretargeting PET (immuno-PET) with an 124I-labeled hapten-peptide. *J Nucl Med.* 2006;47(10):1678-1688.
35. Rossi EA, Goldenberg DM, Cardillo TM, McBride WJ, Sharkey RM, Chang CH. Stably tethered multifunctional structures of defined composition made by the dock and lock method for use in cancer targeting. *Proc Natl Acad Sci U S A.* 2006; 103(18):6841-6846.
36. Rossi EA, Goldenberg DM, Cardillo TM, Stein R, Wang Y, Chang CH. Novel designs of multivalent anti-CD20 humanized antibodies as improved lymphoma therapeutics. *Cancer Res.* 2008; 68(20):8384-8392.
37. Sharkey RM, Karacay H, Cardillo TM, et al. Improving the delivery of radionuclides for imaging and therapy of cancer using pretargeting methods. *Clin Cancer Res.* 2005;11(19):7109S-7121S.
38. Sharkey RM, Karacay H, Vallabhajosula S, et al. Metastatic human colonic carcinoma: molecular imaging with pretargeted SPECT and PET in a mouse model. *Radiology.* 2008;246(2):497-507.
39. Carnahan J, Stein R, Qu Z, et al. Epratuzumab, a CD22-targeting recombinant humanized antibody with a different mode of action from rituximab. *Mol Immunol.* 2007;44(6):1331-1341.
40. Cardarelli PM, Quinn M, Buckman D, et al. Binding to CD20 by anti-B1 antibody or F(ab′)(2) is sufficient for induction of apoptosis in B-cell lines. *Cancer Immunol Immunother.* 2002;51(1):15-24.
41. Glennie MJ, French RR, Cragg MS, Taylor RP. Mechanisms of killing by anti-CD20 monoclonal antibodies. *Mol Immunol.* 2007;44(16):3823-3837.
42. Stein R, Qu Z, Chen S, Solis D, Hansen HJ, Goldenberg DM. Characterization of a humanized IgG4 anti-HLA-DR monoclonal antibody that lacks effector cell functions but retains direct antilymphoma activity and increases the potency of rituximab. *Blood.* 2006;108(8):2736-2744.
43. Goldenberg DM, Rossi EA, Stein R, et al. Properties and structure-function relationships of veltuzumab (hA20), a humanized anti-CD20 monoclonal antibody. *Blood.* 2009;113(5):1062-1070.
44. Belardelli F, Ferrantini M, Proietti E, Kirkwood JM. Interferon-alpha in tumor immunity and immunotherapy. *Cytokine Growth Factor Rev.* 2002;13(2): 119-134.
45. Pelham JM, Gray JD, Flannery GR, Pimm MV, Baldwin RW. Interferon-alpha conjugation to human osteogenic sarcoma monoclonal antibody 791T/36. *Cancer Immunol Immunother.* 1983; 15(3):210-216.
46. Ozzello L, Blank EW, De Rosa CM, et al. Conjugation of interferon alpha to a humanized monoclonal antibody (HuBrE-3vl) enhances the selective localization and antitumor effects of interferon in breast cancer xenografts. *Breast Cancer Res Treat.* 1998;48(2):135-147.
47. Huang TH, Chintalacharuvu KR, Morrison SL. Targeting IFN-alpha to B cell lymphoma by a tumor-specific antibody elicits potent antitumor activities. *J Immunol.* 2007;179(10):6881-6888.
48. Kramer MJ, Dennin R, Kramer C, et al. Cell and virus sensitivity studies with recombinant human alpha interferons. *J Interferon Res.* 1983;3(4): 425-435.
49. Weck PK, Apperson S, May L, Stebbing N. Comparison of the antiviral activities of various cloned human interferon-alpha subtypes in mammalian cell cultures. *J Gen Virol.* 1981;57:233-237.